

Smartphone-based Energy Consumption Simulation for Electric Vehicles

Dipl.-Ing. Benedikt Jäger
Institute of Automotive Technology
Technische Universität München
München, Germany
jaeger@ftm.mw.tum.de

Prof. Dr.-Ing. Markus Lienkamp
Institute of Automotive Technology
Technische Universität München
München, Germany
lienkamp@ftm.mw.tum.de

Abstract—Range anxiety is a major concern related to electric cars' every day applicability. Depending on the individual mobility behavior, electromobility can already make sense today seen from both ecological and economical points of view. In this paper a method to estimate the energy consumption for electric cars in real-time while driving a conventional combustion engine car is presented. The basic idea is to use a smartphone for both data acquisition and as a simulation unit. Based on a parameterized and scalable modeling structure, different vehicle configuration sets can be evaluated easily in real life applications. The proposed simulation is built up as a backward-facing longitudinal dynamic model. The requested energy demand delivered by the traction battery can be calculated based on vehicle motion. Driving resistances, the auxiliary consumer's power requests as well as powertrain efficiency losses are taken in account. Before executing the proposed simulation model, data filtering takes place in real-time on the smartphone. In this paper three different methods for data smoothing are evaluated. Model validation is finally done by means of a standardized NEDC test for four different vehicle models. Additionally, a test drive with an electric car validate the energy consumption model under real-life conditions.

Keywords — *electric vehicle; modeling and simulation; smartphone; energy consumption; smart mobility*

I. MOTIVATION

New mobility concepts have to be developed in the face of increasing energy costs, stricter environmental regulations as well as a growing number of vehicles. Especially non-fossil energy sources are expected to gain more attention in the near future. In this context, electric vehicles can make a contribution to fulfilling customers' daily mobility requirements. Not only technical barriers have to be overcome but also the customers' acceptance needs to increase. Compared to combustion engine vehicles, additional restrictions like the limited range or longer recharging times must be taken in account. That is the reason why each individual mobility behavior has to be analyzed in detail. Required information can be collected with smartphones. In doing so an end user can get an estimation to which degree electromobility is a reasonable solution for his unique mobility pattern. Recommendations for the best matching vehicle configuration can be derived based on the mobility demand. In this context the relationship between energy storage, range and costs can be optimized holistically. One commercial application is a purchase advice for end users. Another use case for OEMs

can be seen as tool in the early vehicle concept development phase. One of the main reasons for customers' skepticism towards electric vehicles is caused by their limited range. However, there is a discrepancy between the really needed and the perceived mobility demand. In [1] the average daily mileage in Germany is stated to be 44 km per person and the average distance per trip is 14.7 km. If the break between two trips is large enough and there is a charging station nearby, the argument of the limited range loses part of its importance. The proposed system approach should address this particular point by analyzing the mobility and the related energy demand.

The basic idea is to simulate electric car behavior while driving in a conventional combustion engine car in real-time on a smartphone. The smartphone is used for sensor data acquisition as well as data processing. Based on the simulation results, the user can get a direct feedback if his individual mobility demand can be fulfilled technically and economically by an electric car. For this purpose the remaining range, the state of charge (SOC) as well as the requested power are calculated in each time step. Here a sufficient accuracy has to be ensured. It is assumed that the driving style and mobility demand will not change dramatically when switching to an electric car.

Various vehicle and also charging infrastructure configurations can be viewed and treated integrally in a short time. A virtual fleet test can be designed by connecting several single vehicle simulations. This approach saves time and money compared to a conventional fleet test with real cars.

After presenting fundamentals of vehicle system modeling in section II, the state of the art in relation to electric car simulation on smartphones will be presented in section III, followed by a more detail description of an electric vehicle model in section IV. Data acquisition and data preparation issues related to smartphone devices are shown in section V. In section VI, the proposed simulation model is validated using both an NEDC-cycle and a test drive in a real electric car.

II. FUNDAMENTALS OF VEHICLE SYSTEMS MODELING

Simulation models can be divided into steady-state, quasi-steady and dynamic ones [2]. Depending on its application purpose, individual levels of detail are needed to represent the relevant system behavior. Steady-state and quasi-steady models have the benefit of needing less computation effort compared to dynamic simulations. However, this leads to more inaccurate

results if states outside the chosen operating point are regarded. Typically, physically-based models can represent the dynamic behavior in a broad operation field within different time scales. This feature is important when analyzing component interactions, like it is needed for optimization purposes on component level. Generalized mobility analysis focuses more on a global view, for example on the entire vehicle energy consumption. In this case it is more important to represent the component's energy efficiency instead of modeling all detailed component interactions.

Another distinction of vehicle models can be derived seen from its calculation point of view. There are forward looking models and backward facing models. [2]

When using a backward facing approach, the relationship between cause and effect is turned around. This means the vehicle's velocity and acceleration is used as input for calculating the operation points step-by-step for the following components. A causal loop through the drivetrain for an electric car is like wheel, transmission, clutch, electric drive and traction battery. For this type of approach no driver model is needed and the calculation effort is minimized. Efficiency maps for vehicle components can be estimated or are provided by manufactures. This way the energy flow inside the vehicle can be simulated efficiently. Problems can arise during a simulation execution if components run in restriction, like physical constraints. Besides, efficiency maps are generated during steady-state testing. So dynamic effects cannot be represented.

A forward-looking approach is based on a control loop that uses a driver model as a controller for the given velocity. Here the components' operation points are adjusted according to the drivers' feedback. Typically, the accelerator and brake pedal positions are used to minimize the error between the driver request and the actual vehicle response. In a simple realization a PI controller is used to control the speed. The engine torque needed is calculated based on the accelerator/brake pedal signal. Finally, efficiency losses in the drivetrain influence the traction force which can be transferred to the tire/road surface. Forward simulations are often used for developing control strategies or x-in-the-loop applications. Because the simulation model is based on equations using vehicle states, the computational effort is higher compared to a backward-facing approach [3].

III. RELATED WORK

In the last decade, modeling and simulation has become a key factor inside the vehicle development process because simulation can save both money and time. Even results that cannot be measured in a running system may be provided by simulations. The field of application ranges from traditional vehicle dynamics and safety investigation to construction issues or cost evaluations.

Most smartphone applications for electric cars being published extend the common vehicle-driver interface. Standard functions are controlling of air conditioning or heating systems, observing the battery's state of charge, fuel level or parking location. For electric cars there are also options to monitor a running charging process.

The smartphone application iEV [4] is focused on simulating electric cars while driving in a conventional combustion engine car. The user can choose 10 different preselected vehicle types.

Input data needed is provided by the GPS sensor inside the smartphone. After finishing one trip, the user gets informed about the consumed energy and the trip distance and time as well as the chosen route. According to [4] driving speed, road inclination, regenerative braking, auxiliary power and both heating as well as cooling demands according to the actual temperature are taken into account to estimate electric car energy consumption. In contrast to this paper, there is no option to create a user-defined parameter set for the vehicle model. Moreover the charging behavior is not considered in [4].

mapZero [5] is an application focused on estimating the remaining range of electric cars, bikes or pedelecs. The user can choose his/her favorite vehicle type from a database with more than 50 predefined vehicles. Based on the current smartphone position the remaining range is calculated in the cloud using map-based geographic information system information. The factors taken into account are battery capacity, air and roll resistance, as well as the current outdoor temperature or the driving style. In order to extend GPS data, mapZero permits the connection of an external obd2-bluetooth adapter to the smartphone and so the collection and processing of internal vehicle information. Vehicle charging is not considered.

BMW Evolve [6] provided by BMW is another application to simulate an electric car under real conditions. By analyzing each individual driving pattern via GPS, the user gets an estimation if an electric car matches his mobility requirements. A virtual vehicle state (driving, parking or charging) must be selected by the user in order to control the virtual car.

eWolf [7] is a smartphone application to estimate the range of electric cars based on a chosen vehicle configuration. As input the average speed must be set by the user. No sensor and travel data from the smartphone is used. The changeable parameters are the front surface, the drag coefficient, the vehicle mass, traction battery size as well as additional auxiliary consumers. The system does not provide an individual mobility analysis.

IV. ELECTRIC VEHICLE MODELING AND SIMULATION PACKAGE

In this section the basic modeling design for the electric vehicle simulation executable on smartphones is presented. The primary goal is to build up a modular energy consumption model for several types of electric vehicles. The model is mainly based on power flow interfaces describing quasi-steady state conditions. A backward-facing simulation is chosen due to its reduced computational effort and simple system structure. The model is divided into system parameters and state variables. Parameters describe constants whereas state variables characterize the dynamic behavior.

In total three overall vehicle states are defined: driving, charging and parking. Input variables during driving are set to

- vehicle position
- longitudinal velocity
- longitudinal acceleration
- altitude above sea level

Both remaining range and state-of-charge of the chosen electric vehicle are output variables of the simulation system. Fig. 1

shows the internal structure of the backward facing model. Different calculations take place according to the vehicle state. The vehicle body is considered as point mass. When moving, first the driving resistance equations are calculated followed by a powertrain energy loss estimation. The total energy demand taken from the battery is determined by the sum of the powertrain and the auxiliary consumers' power requests. The total electric energy transferred during a charging process is specified by the charging station's power supply.

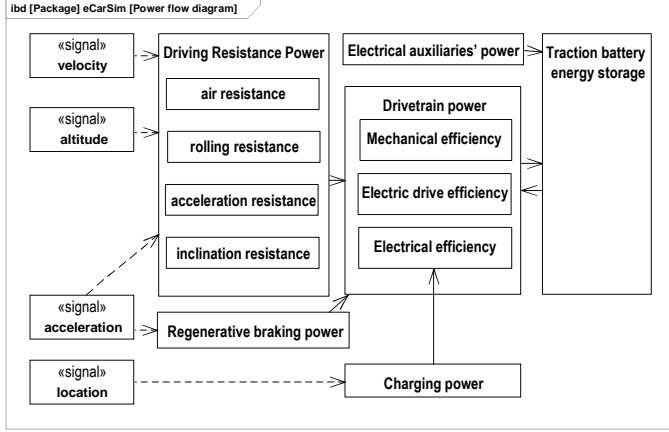


Fig. 1. Basic structure of energy flow model (backward facing model)

There are two options to get energy back into the traction battery. First, energy can be regenerated by using the electric drive as a generator for braking. Secondly, the vehicle is charged at a charging station.

The total power that has to be provided by the traction battery P_{req} is calculated from:

$$P_{req} = P_d + P_{reg} + P_{aux} = \frac{P_{res}}{\eta} + P_{reg} + P_{aux} \quad (1)$$

- P_{req} = total requested power from the battery
- P_d = total power demand by powertrain
- P_{reg} = total recuperated power
- P_{aux} = total power demand by auxiliary consumers
- P_{res} = total driving resistance power
- $\eta = \eta_e * \eta_m * \eta_d$ = overall powertrain efficiency
- η_e = electrical powertrain efficiency
- η_m = mechanical powertrain efficiency
- η_d = electric drive efficiency

The energy taken from or feed back into the battery is calculated by multiplying P_{req} with the usage time t :

$$\Delta E = P_{req} \cdot t \quad (2)$$

This amount of energy is stored as kinetic energy during driving, as potential energy after altitude changes or is dissipated in the form of mechanical energy losses. There are mainly aerodynamic friction losses, rolling friction losses and

braking losses [8]. Equations to calculate these driving resistances are presented in the next subsections. Assumptions made here are described in detail in [9].

A. Driving resistance

When moving, driving resistances counteract against the propulsion power as illustrated in Fig. 2. Here P_{res} is defined as the sum of all resistance forces multiplied by the vehicle velocity v :

$$P_{res} = \sum F_{res} \cdot v = (F_{hc} + F_{rr} + F_{ad} + F_i) \cdot v \quad (3)$$

- F_{hc} = hill climbing force
- F_{rr} = rolling friction force
- F_{ad} = aerodynamic drag force
- F_i = inert force

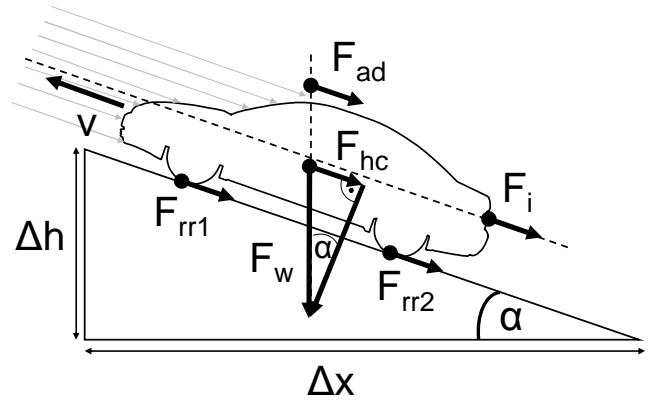


Fig. 2. Driving resistance illustration

Caused by the downhill force the hill climbing force F_{hc} is orientated parallel to the driving direction. Its calculation is described in equation (4). Based on the driven distance Δx and altitude difference Δh the road incline α is defined as equation (5).

$$F_{hc} = F_w \cdot \sin \alpha = m_{ent} \cdot g \cdot \sin \alpha \quad (4)$$

$$\alpha = \arcsin\left(\frac{\Delta h}{\Delta x}\right) \quad (5)$$

m_{ent} = entire vehicle mass

Substantial energy losses are caused by the rolling resistance. The reason for the tire deformation is the vehicle mass m_{ent} or the elasticity of the tire material. Most energy is being lost in the form of heat [10]. The rolling resistance is calculated as (6):

$$F_{rr} = F_w \cdot \cos \alpha \cdot f_R = m_{ent} \cdot g \cdot \cos \alpha \cdot f_R \quad (6)$$

f_R = rolling resistance coefficient

Because the vehicle weight, aligned to the road, is causing a deformation of the tire, the road incline α has to be considered. The roll resistance coefficient depends on factors like the tire

pressure, tire temperature, tire blend, tread or vehicle velocity. Under slow driving conditions, the rolling resistance coefficient can be considered as nearly constant. The resistance increases progressively when driving faster on made-up roads. The reasons are said to be wave formation and tire heating [10]. Energy losses due to aerodynamic drag force F_{ad} increase in a square ratio with the vehicle speed. At high vehicle speeds F_{ad} causes a major part of the total driving resistance. The force can be described as the effort the vehicle has to overcome against the surrounding ambient air medium. When driving, this force is generated by pressure difference, swirl and surface friction on the vehicle body. F_{ad} can be calculated like (7):

$$F_{ad} = \frac{1}{2} \cdot \rho_{air} \cdot c_w \cdot A_{fs} \cdot v^2 \quad (7)$$

- ρ_{air} = density of the ambient air
- c_w = drag coefficient
- A_{fs} = front surface of the vehicle

Characterized by the vehicle design, the c_w -value is determined by experiment or simulation. In equation (7) only flows in the longitudinal direction are considered. Crosswinds are not regarded in this type of modeling [10].

The inert force F_i is described in Newton's second law of motion. A force has to be applied to a body when it should be accelerated. Translational acceleration is influenced by the entire vehicle mass whereas rotatory accelerations have to be considered at wheels, tires as well as power transmission parts like drive shafts or gear wheels. As it is hard to describe all rotatory inertial and transmission in a vehicle, a global factor ϵ is introduced to represent its effects. ϵ mainly depends on the chosen gear steps and gear ratios [9]. By doing so the total acceleration force F_i is defined as (8):

$$F_i = m_{ent} \cdot \epsilon \cdot a \quad (8)$$

- ϵ = factor for rotatory and translational movements
- a = longitudinal acceleration

B. Powertrain

Mechanical and electrical losses and losses inside the electric drive influence the total powertrain efficiency. Mechanical losses are primarily caused by slippage in propulsion components and transmission, axle differentials, and friction losses. Due to a wide variety of mechanical designs and complex modeling efforts, it is hard to simulate mechanical components in detail.

1) Battery & power electronics

Units, traction battery and power electronics effect electric efficiency. Power electronics provide the electrical interface to connect electrical components inside the car. This means to transform operation voltages into the desired mode and level. As an example DC voltage provided by the traction battery has to be transferred into AC voltage in order to run alternating current machines, like an asynchronous machine. For regeneration purposes, AC voltage provided by the electric drive has to be

rectified to charge the traction battery. DC/DC converters in electric cars are commonly used to feed auxiliary consumers from high voltage energy reservoirs. For charging AC voltage, supplied by the mains, has to be transformed into DC voltage required by the traction battery. Charging modules made of power electronics perform this task inside or outside the car. All transformation processes involve a degree of energy loss. For simplification in this paper a constant total electric efficiency of 0.9 is assumed as published in [11].

2) Electric drive

Losses inside an electric drive strongly depend on both torque load and rotational speed. If the current load level is known, efficiency maps can be used to estimate losses inside the machine. Besides the maximum regenerative power is determined by its physical constraints. Efficiency maps are generated by running an electric drive under various steady-state operation points. Because characteristic diagrams are obtained by experiment, efficiency maps for individual power classes and machine types have to be interpolated as described in [12]. For our approach, interpolation is done on the basis of various efficiency maps stored in a database. By choosing the desired drive power and machine type a search algorithm finds the two closest characteristic diagrams. Map scaling is achieved using information about the maximum rotational speed, the maximum torque and maximum electric drive power. The rotational drive speed can be calculated based on longitudinal vehicle speed, gear ratio and tire diameter. While knowing the requested drive power and the machine's rotational speed n , the corresponding torque T and the electric drive efficiency are determined as shown in Fig. 3.

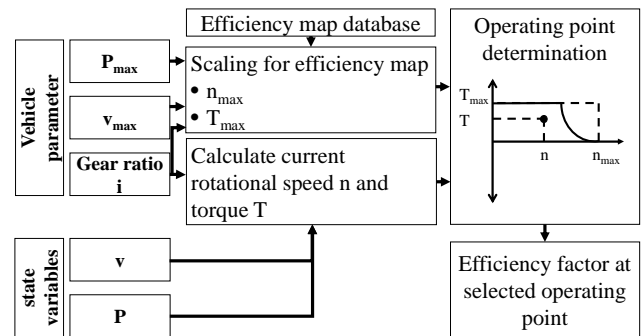


Fig. 3. Algorithm for electric drive efficiency

3) Regenerative braking

Basically, there are two different modes of regenerative braking. The electric drive simulates the drag torque of a common combustion engine or acts as an additional vehicle brake component. The maximum regenerated power is limited by the chosen electric drive, the level of deceleration, the traction potential of the wheels as well as the charge acceptance of the traction battery. According to the chosen battery technology, charging power is limited due to lifecycle regression. If the driver requests a higher deceleration than can be provided by the electric drive, a further braking system has to ensure deceleration. In order to specify the recuperated power in a simulation, the following aspects need to be considered. One key factor is given by the driving resistances. Since this force acts in

the opposite direction to the propulsion power, a vehicle is automatically decelerated to a certain amount. Additionally, under slow vehicle speed conditions maximum regenerated power is limited by the electric drive's operation point. The amount of energy to be recovered is further reduced by efficiency losses inside powertrain components. As mentioned in [13] only 44% of the maximum regenerated potential can be regained when passing a New European Driving Cycle (NEDC) with a luxury-segment vehicle. To simplify matters, the maximum regeneration factor is set as a fixed parameter as given in [13].

C. Auxiliary consumers

Electrical consumers have a great impact on the vehicle range. Especially heating and air conditioning systems cause a sizeable share of the energy consumption. Average power demands reach up to 5 kW per component [14]. Lighting or entertainment systems affect the vehicle's power demand as well. The amount of energy requested strongly depends on the built-in equipment but also on other factors like car body color and the associated absorption coefficient. Due to the fact that common car users have no knowledge about the energy demand and it can not be measured directly with smartphones, average energy consumption values for single auxiliary consumers are used. The user has to select a discrete power level for the heating and air conditioning system manually. This way the weather and temperature influence is represented in the form of an additional auxiliary power demand.

V. VALIDATION OF SMARTPHONE INPUT DATA

The next step after building the model is to get reliable input data for the simulation execution in real-time. That's why first features of build-in sensors of modern smartphones are presented followed by the real-time data filtering algorithm.

A. Smartphone sensors

Depending on the chosen model, smartphones are equipped with different sensors. Table I gives an overview of main sensor classifications.

TABLE I. CLASSES OF SMARTPHONE SENSORS

| Sensor class | Sensor type |
|-----------------------|--|
| Motion sensors | <ul style="list-style-type: none"> • Accelerometer • Gravity sensor • Gyroscope • Rotational vector sensor |
| Environmental sensors | <ul style="list-style-type: none"> • Barometer • Photometer • Thermometer |
| Position sensors | <ul style="list-style-type: none"> • Orientation sensor • Magnetometer |

Motion sensors measure acceleration and rotational forces. Ambient temperature, air pressure and illumination are provided by environmental sensors. Position sensors determine the smartphone position inside the fixed-in-the-earth coordinate system. For executing the simulation model proposed in section IV in a moving car, the vehicle longitudinal velocity, acceleration and the road inclination need to be measured. Location and velocity are provided by the built-in GPS sensor.

The vehicle's longitudinal acceleration can be gathered with either the accelerometer or the GPS sensor. If using the GPS signal, longitudinal acceleration is calculated as a derivation of the velocity. The more direct way is to use the integrated accelerometer sensor. Because the smartphone coordinate system commonly mismatches with the vehicle's coordinate system, a coordination transformation has to take place. For this transformation the orientation of the smartphone relative to the vehicle is needed. With the aid of a calibration run, the smartphone orientation can be estimated. In this process the vehicle must be brought into a predefined condition (e.g. no external acceleration, flat area). As the proposed system should work without any calibration effort, the vehicle acceleration measurement is realized using the GPS sensor.

Road incline estimation can be done with the aid of the GPS altitude signal, air pressure measurements or map-based. In all cases, the signal's accuracy is limited by the finite sample rate defined by each sensor module. The maximum sample rate of a GPS sensor on mobile devices is commonly specified by 1 Hz. Thus there's a staircase-shaped velocity signal that has to be smoothed with suitable filter methods [15].

Digital filters are categorized into Finite Impulse Response (FIR) and Infinite Impulse Response (IIR) filters. IIR-filters use both feedback values from the past as well as new gathered signal data. As a possible realization of a FIR-filter a simple moving average filter is applied. Additionally exponential moving average as well as double exponential smoothing filter designs are evaluated as examples of IIR types.

B. Data filtering methodology

One of the most common smoothing algorithms is given by the simple moving average filter. If applying an unweighted version, the calculation is done as described in [16] from (9):

$$s_{ma,t} = \frac{1}{k} \cdot \sum_{n=0}^{k-1} x_{t-n} = \frac{(x_t + x_{t-1} + \dots + x_{t-k+1})}{k} \quad (9)$$

Index t represents the current time step. x is the unfiltered sensor value. Parameter k defines the filter order and thus the moving window size. Both smoothness and response time strongly depend on the chosen k.

Exponential moving average filters are composed as shown in equation (10):

$$s_t = s_{t-1} \cdot (1 - \alpha) + \alpha \cdot x_t \quad (10)$$

- s_t = new smoothed output
- s_{t-1} = previous smoothed output
- α = smoothing factor ([0,1])
- x_t = new unfiltered data

New unfiltered data x_t is weighted with respect to the previous filtered data. The chosen smoothing factor α strongly influences the response time of the filter. If α is set too low, noise reduction is done adequately but the response time is delayed. If α is chosen too high, filtering does not lead to the expected effect. Double exponential smoothing filtering is a method widely used for filtering continuously increasing or decreasing signals.

Based on the curve gradient, a new data point is estimated and the response time is kept constant. [17]

All calculation steps needed are shown in equation (11), (12) and (13):

$$s_{1,t} = s_{1,t-1} \cdot (1 - \alpha) + \alpha \cdot x_t \quad (11)$$

$$s_{2,t} = s_{2,t-1} \cdot (1 - \alpha) + \alpha \cdot s_{1,t} \quad (12)$$

$$s_0 = 2 \cdot s_{1,t} - s_{2,t} \quad (13)$$

s_0 = predicted value

C. Filter design by experiment

In order to find suitable filter coefficients and to assess different filter qualities related to individual sensor signals, a test drive has been performed. The chosen route around Garching, Germany had a distance of about 10 kilometers (equal parts of highway, country road and city road). Apart from the smartphone, reference data is collected by means of an OXTS RT3003 inertial navigation system. Both vehicle velocity and 3D acceleration are tracked by each sensor system independently. The smartphone is attached on top of the inertial navigation system housing, so both coordinate systems can be aligned easily. The test vehicle was an Audi Q7 and the smartphone was a Samsung Galaxy S III.

To carry out a proper valuation between both measurement systems, a least square method is applied. This approach is commonly applied for compliance tests of functions or data. By summing up the square error between the reference and measured value, an evaluation of two data sets is carried out. Larger differences are weighted more strongly. Fig. 4 illustrates the vehicle velocity recorded by the reference system.

A detailed evaluation of all three previously proposed filtering algorithms can be performed on the basis of the test. A minimum error configuration was worked out by changing the filter coefficients (k or α) for each method. Here the coefficient with the smallest error sum is chosen. In our test set the best results for filtering the vehicle velocity were obtained using a simple average filter. Fig. 5 illustrates the filtered and unfiltered velocity signal. The sum of least square calculation versus the window size is shown in Fig. 6.

In the test ride, the best results were obtained when applying an exponential moving average filter for acceleration data. Table II gives an overview of the calculated least square errors. Based on the results, the input data filtering is performed in real-time before executing the vehicle simulation model.

TABLE II. LEAST SQUARE ERRORS FOR VELOCITY AND ACCELERATION

| Signal | simple moving average filter | exponential moving average filter | Double exponential smoothing filter |
|--|--|---|--|
| Velocity (filter coefficient) | 1886 (m/s) ² (k = 4) | 2131 (m/s) ² (α = 0.183) | 2410 (m/s) ² (α = 0.2) |
| Longitudinal acceleration (filter coefficient) | 145 (m/s ²) ² (k = 6) | 121 (m/s ²) ² (α = 0.28) | 142 (m/s ²) ² (α = 0.159) |

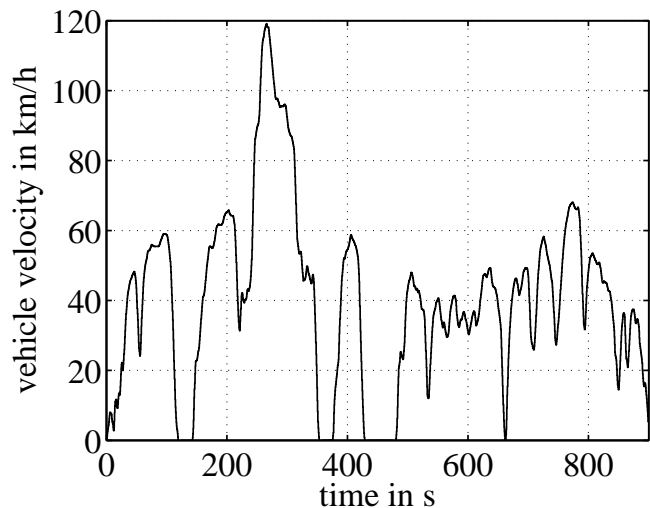


Fig. 4. Reference velocity recorded using inertial navigation system

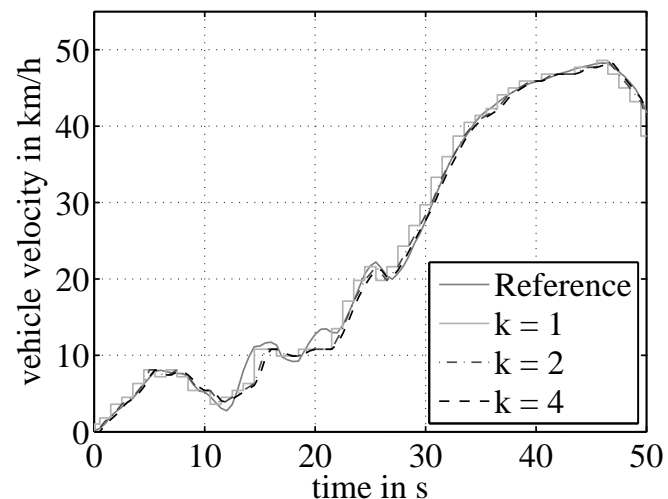


Fig. 5. Different filter orders of moving average filter applied to velocity signal

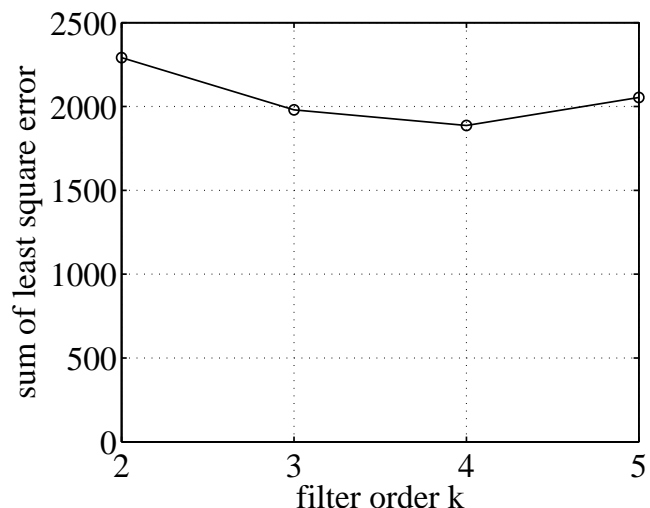


Fig. 6. Least square error versus filter order for designing the filter

VI. VALIDATION OF THE SIMULATION MODEL

Two different ways of validation are suggested to check the validity of the vehicle simulation model proposed in section IV. First, a comparison between energy consumption specifications given by manufacturers and the simulation model is presented. Second, a test drive using an electric car is performed.

A. Offline NEDC-cycle

The standardized NEDC cycle is used to compare the energy consumption of different vehicles. According to the European standard ECE R101 [18], losses occurring during charging are taken into account for energy consumption determination. Efficiency losses are caused by the charging module, cables or the traction battery. That is why the vehicle is fully charged after each single test cycle run. In the proposed simulation, those losses are represented by the electric efficiency except for losses caused by external charging stations.

Parameterization has to take place before running the simulation. For further investigations parameters shown in table III are kept constant, whereas the rest of the parameters are varied according to the chosen vehicle model.

TABLE III. FIXED PARAMETER SET USED IN SIMULATION

| Parameter | Value |
|---|-------|
| Rolling resistance coefficient | 0.01 |
| Recuperation factor during deceleration | 61 % |
| Electrical efficiency | 90 % |
| Mechanical efficiency | 90 % |
| Tire diameter | 0.6 m |
| Velocity filter coefficient | 4 |
| Acceleration filter coefficient | 0.28 |

If car manufactures do not provide information about required vehicle parameters, estimated values are used. For example, the gear ratio can be calculated with knowledge of the maximum vehicle velocity and the maximum electric drive rotational speed. In total, four different vehicle parameter sets are investigated in this paper (see table IV).

Results of one NEDC simulation execution are shown in table V. It can be seen that the largest energy consumption difference (Renault Kangoo Maxi Z.E.) is about 9.8%. One reason for this gap could be found in an inaccurate energy consumption specification provided by the manufacturer. The energy consumption for all Renault Kangoo models is officially declared to be the same even though the “Maxi” version weighs 127 kg more compared to its lightweight version. The most precise estimation is obtained for the Renault ZOE with a difference of 1.2%.

The average variation of all four simulation runs is 4.95%. This discrepancy can be explained partially by non-considered efficiency losses during recharging. In Fig. 7 the requested total power of one NEDC simulation run (Mitsubishi iMiEV) is displayed. Fig. 8 and Fig. 9 illustrate the power distribution with respect to the driving resistance.

TABLE IV. INDIVIDUAL VEHICLE PARAMETER SET USED IN SIMULATION

| Parameter | Mitsubishi i-MiEV | Renault ZOE | Nissan LEAF | Renault Kangoo Maxi Z.E. |
|--|-------------------|---------------------|-------------|--------------------------|
| Traction battery capacity [kW] | 16 | 22 | 24 | 22 |
| Unloaded weight [kg] | 1110 | 1503 | 1545 | 1628 |
| Front surface [m ²] _a | 2.14 | 2.2 | 2.27 | 2.69 |
| c_w -value [-] ^a | 0.33 | 0.29 | 0.29 | 0.33 |
| Throwing body factor [-] ^a | 1.1 | 1.15 | 1.16 | 1.2 |
| Gear ratio [-] | 6.066:1 | 9.47:1 ^a | 7.94 | 10.4:1 ^a |
| Top speed [km/h] | 130 | 135 | 145 | 130 |
| Drive power [kW] | 49 | 43 | 80 | 44 |
| Range in NEDC simulation [km] | 150 | 210 | 175 | 170 |

^a Estimated value

TABLE V. ENERGY CONSUMPTION IN NEDC SIMULATION

| Vehicle | Average energy consumption E_{con} in Wh/km | | |
|------------------|---|---------------------|-----------------------|
| | Simulation | Manufacturer's data | ΔE_{con} in % |
| Mitsubishi iMiEV | 133 | 135 | -1.3 |
| Renault ZOE | 144 | 146 | -1.2 |
| Nissan Leaf | 160 | 173 | -7.5 |
| Kangoo Maxi Z.E. | 170 | 155 | + 9.8 |

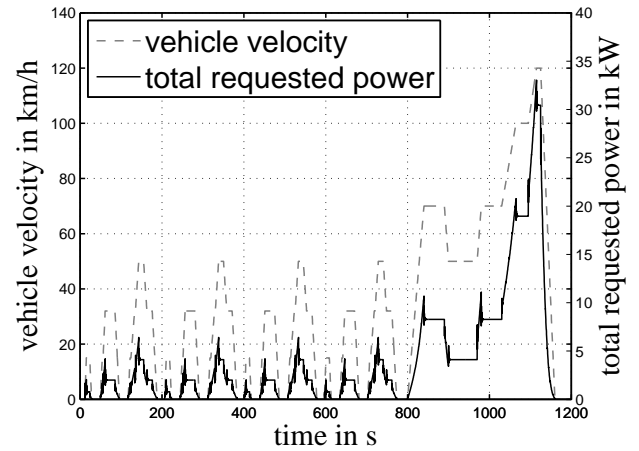


Fig. 7. Power demand due to air and rolling resistance

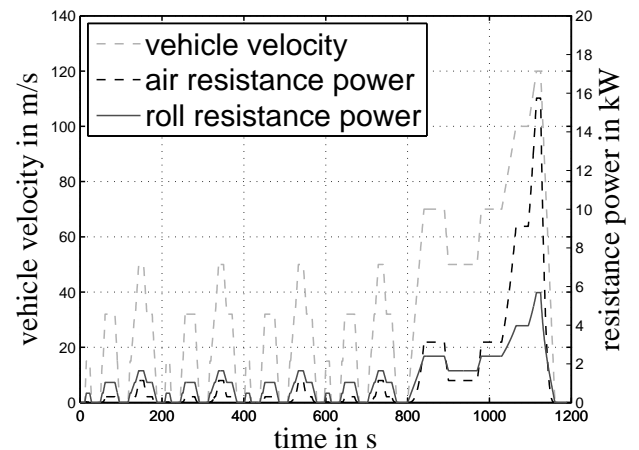


Fig. 8. Power demand due to air and roll resistance

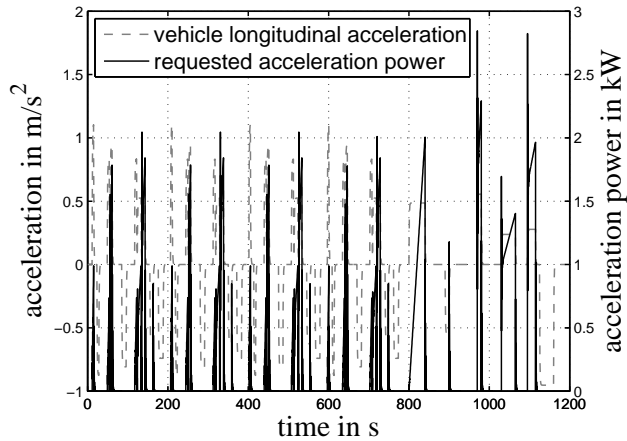


Fig. 9. Power demand due to acceleration resistance

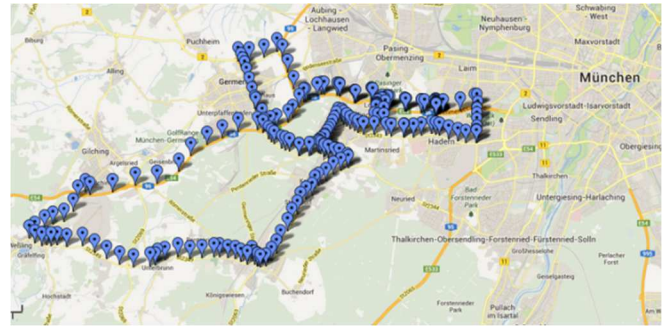


Fig. 10. Test route chosen for validation (map by google)

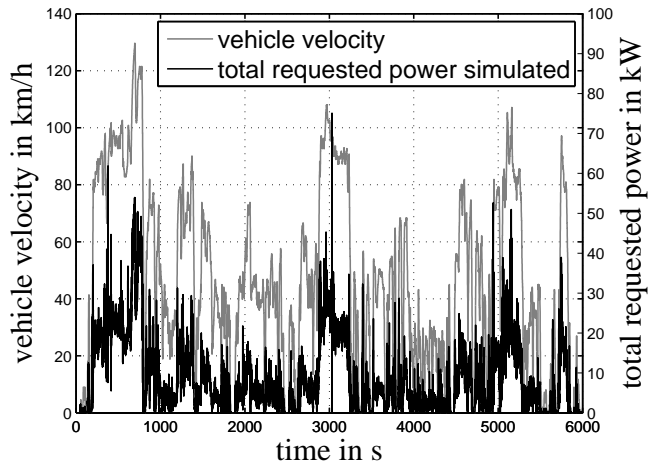


Fig. 11. Speed profile and simulated power demand of test trip

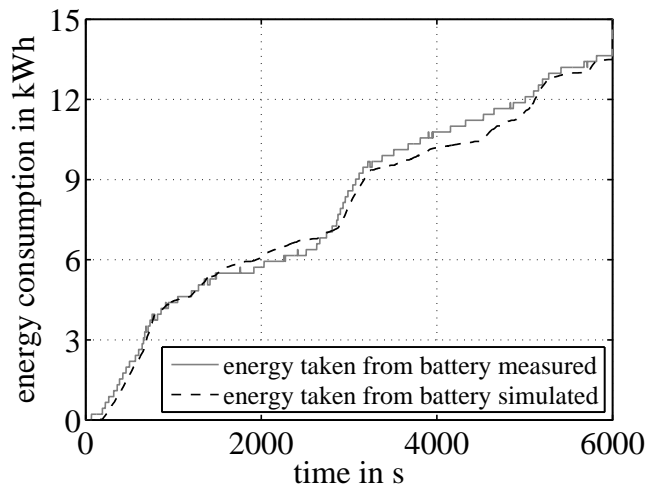


Fig. 12. Comparison between simulated and measured energy consumption

B. Online test ride

Results from a test ride with an electric Renault Kangoo Maxi Z.E. are presented in the following. The vehicle's CAN interface is logged in order to get reference data for comparison. In doing so the state-of-charge estimation provided by the simulation can be evaluated with experimental data. The parameter set selected for the simulation is given in table IV. The Samsung Galaxy S III is used for data acquisition and computational purposes. The chosen route is illustrated in Fig. 10. The trip consists of one third highway, one third country road and one third city road with a total distance of 77.1 km. The total driving time lasts about 100 minutes. The state-of-charge at the trip start was 81% and at the end it was 19%. Lighting, radio, heating or air conditioning were turned off during the test drive. The measured vehicle velocity and the calculated total power demand are shown in Fig. 11. The absolute energy consumption deviation at end of the test is 0.78% as shown in Fig. 12. The largest difference between the simulated and measured energy consumption during the test ride is 7.3%. This error especially occurs at low vehicle speed.

VII. CONCLUSION

A smartphone-based energy consumption model for electric cars was presented in this paper. After describing the main modeling structure with its key components, data acquisition and preparation issues related to smartphone were investigated. As a result, both the vehicle velocity and acceleration can be assessed using the smartphone's GPS sensor and adequate data filtering methods. Velocity signals can be smoothed using a simple moving average filter. For acceleration signals an exponential moving average filter gave the best performance. Finally, the proposed electric vehicle model is validated by means of a standardized NEDC test cycle and data from the manufacturer. A test drive with an electric car evaluated the proposed energy consumption model under real-life conditions. No additional hardware or data interfaces are needed to run the simulation apart from a smartphone. The proposed system is the first electric car simulation running in real time on smartphones featuring a fully parametrizable and scalable vehicle model.

ACKNOWLEDGMENT

This work was funded by the German Federal Ministry for Economic Affairs and Energy (Project VEM; 01MF12111).

REFERENCES

- [1] infas, DLR, "Mobilität in Deutschland 2008 - Ergebnisbericht," BMVBS, Luxembourg, 2010.
- [2] D. W. Gao, "Modeling and Simulation of Electric and Hybrid Vehicles," *Proceedings of the IEEE Volume: 95 Issue: 4*, pp. 729-745, 30 04 2007.
- [3] T. Markel, A. Brooker, T. Hendricks, V. Johnson, K. Kelly, B. Kramer, M. O'Keefe, S. Sprik and K. Wipke, "ADVISOR: a systems analysis tool for advanced vehicle modeling," *Journal of Power Sources Volume 110 Issue 2*, pp. 255-266, 22 08 2002.
- [4] O. T. Mezger, "iEV App," Green & Energy GmbH, [Online]. Available: <http://www.ievapp.com/>. [Accessed 31 01 2014].
- [5] P. Conradi, P. Bouteiller and S. Hanßen, "Dynamic Cruising Range Prediction for Electric Vehicles," in *VDI - Advanced Microsystems for Automotive Applications 2011*, Berlin Heidelberg, Springer, 2011, pp. 269-277.
- [6] BMW of North America, "BMW EVolve App," BMW, 25 07 2011. [Online]. Available: <https://play.google.com/store/apps/details?id=com.bmw.activities>. [Accessed 14 01 2014].
- [7] "e-Wolf for iPhone, iPod touch und iPad," e-Wolf GmbH, 17 02 2010. [Online]. Available: <https://itunes.apple.com/de/app/e-wolf/id355398874?mt=8>. [Accessed 31 1 2014].
- [8] L. Guzzella and A. Sciarretta, *Vehicle Propulsion Systems*, Berlin Heidelberg: Springer, 2013.
- [9] K.-L. Haken, *Grundlagen der Kraftfahrzeugtechnik*, München: Carl Hanser Verlag, 2008.
- [10] M. Mitschke and H. Wallentowitz, *Dynamik der Straßenfahrzeuge*, Berlin Heidelberg: Springer, 2004.
- [11] M. Lienkamp, *Elektromobilität: Hype oder Revolution*, Springer Vieweg, 2012, ISBN 978-3642285486.
- [12] T. Pesce, "Ein Werkzeug zur Spezifikation von effizienten Antriebstopologien für Elektrofahrzeuge," Dissertation, Technische Universität München, Lehrstuhl für Fahrzeugtechnik, München, 2014.
- [13] P. Hofmann, *Hybridfahrzeuge: Ein alternatives Antriebskonzept für die Zukunft*, Wien: Springer, 2010.
- [14] K. Umezumi and H. Noyama, "Air-Conditioning system For Electric Vehicles," in *SAE Automotive Refrigerant & System Efficiency Symposium 2010*, Scottsdale, Arizona, 2010.
- [15] G. Milete and A. Stroud, *Professional Android Sensor Programming*, Crosspoint Boulevard: Wiley, 2012.
- [16] J. G. Proakis and D. G. Manolakis, *Digital Signal Processing*, Upper Saddle River, New Jersey: Simon & Schuster/A Viacom Company, 1996, ISBN 0-13-394338-9.
- [17] G. Schulte, *Material- und Logistikmanagement*, München: Oldenbourg Wissenschaftsverlag GmbH, 2001, ISBN 3-486-25458-8.
- [18] UN ECE, "Regelung Nr. 101," in *Amtsblatt der Europäischen Union*, 2012, p. L 138.